

# CODEX-b: Opening New Windows to the Long-Lived Particle Frontier at the LHC

ESPP Update

## Comprehensive summary

Giulio Aielli <sup>1</sup>, Juliette Alimena <sup>2</sup>, Saul Balcarcel-Salazar <sup>3</sup>, Eli Ben Haim <sup>4</sup>, András Barnabás Burucs <sup>5</sup>, Roberto Cardarelli <sup>1</sup>, Matthew J. Charles <sup>4</sup>, Xabier Cid Vidal <sup>6</sup>, Albert De Roeck <sup>7</sup>, Biplab Dey <sup>5</sup>, Silviu Dobrescu <sup>8</sup>, Ozgur Durmus <sup>5</sup>, Mohamed Elashri <sup>8</sup>, Vladimir V. Gligorov <sup>4</sup>, Rebeca Gonzalez Suarez <sup>9</sup>, Zarría Gray <sup>8</sup>, Conor Henderson <sup>8</sup>, Louis Henry <sup>10</sup>, Philip Ilten <sup>8</sup>, Daniel Johnson <sup>11</sup>, Jacob Kautz <sup>8</sup>, Simon Knapen <sup>12,13</sup>, Bingxuan Liu <sup>14</sup>, Yang Liu <sup>14</sup>, Saul López Soliño <sup>6</sup>, Pablo Eduardo Menéndez-Valdés Pérez <sup>6</sup>, Titus Mombächer <sup>7</sup>, Benjamin Nachman <sup>12</sup>, David T. Northacker <sup>8</sup>, Gabriel M. Nowak <sup>8</sup>, Michele Papucci <sup>15</sup>, Gabriella Pásztor <sup>5</sup>, María Pereira Martínez <sup>6</sup>, Michael Peters <sup>8</sup>, Jake Pfaller <sup>8</sup>, Luca Pizzimento <sup>16</sup>, Máximo Pló Casasús <sup>6</sup>, Gian Andrea Rassati <sup>8</sup>, Dean J. Robinson <sup>12,13</sup>, Emilio Xosé Rodríguez Fernández <sup>6</sup>, Debashis Sahoo <sup>5</sup>, Sinem Simsek <sup>17</sup>, Michael D. Sokoloff <sup>8</sup>, Joéal Subash <sup>11</sup>, James Swanson <sup>8</sup>, Abhinaba Upadhyay <sup>5</sup>, Riccardo Vari <sup>18</sup>, Carlos Vázquez Sierra <sup>19</sup>, Gábor Veres <sup>5</sup>, Nigel Watson <sup>11</sup>, Michael K. Wilkinson <sup>8</sup>, Michael Williams <sup>3</sup> and Eleanor Winkler <sup>3</sup>

(CODEX-b collaboration)

<sup>1</sup> *Università e INFN Sezione di Roma Tor Vergata, Roma, Italy*

<sup>2</sup> *Deutsches Elektronen-Synchrotron (DESY), Hamburg, Germany*

<sup>3</sup> *Laboratory for Nuclear Science, Massachusetts Institute of Technology, Cambridge, MA 02139, USA*

<sup>4</sup> *LPNHE, Sorbonne Université, Université Paris Cité, CNRS/IN2P3, Paris, France*

<sup>5</sup> *ELTE Eötvös Loránd University, Budapest, Hungary*

<sup>6</sup> *Instituto Galego de Física de Altas Enerxías (IGFAE),*

*Universidade de Santiago de Compostela, Santiago de Compostela, Spain*

<sup>7</sup> *European Organization for Nuclear Research (CERN), Geneva, Switzerland*

<sup>8</sup> *Department of Physics, University of Cincinnati, Cincinnati, OH 45221, USA*

<sup>9</sup> *Department of Physics and Astronomy, Uppsala Universitet, Uppsala, Sweden*

<sup>10</sup> *Ecole Polytechnique Fédérale Lausanne, Lausanne, Switzerland*

<sup>11</sup> *University of Birmingham, Birmingham, United Kingdom*

<sup>12</sup> *Physics Division, Lawrence Berkeley National Laboratory, Berkeley, CA 94720, USA*

<sup>13</sup> *Department of Physics, University of California, Berkeley, CA 94720, USA*

<sup>14</sup> *School of Science, Shenzhen Campus of Sun Yat-Sen University, Shenzhen, China*

<sup>15</sup> *Walter Burke Institute for Theoretical Physics,*

*California Institute of Technology, Pasadena, CA 91125, USA*

<sup>16</sup> *University of Hong Kong, Hong Kong*

<sup>17</sup> *Istinye University, Istanbul, Turkey*

<sup>18</sup> *INFN Sezione di Roma La Sapienza, Roma, Italy*

<sup>19</sup> *Universidade da Coruña, A Coruña, Galicia, Spain*

This document is written as a contribution to the European Strategy of Particle Physics (ESPP) update. We offer a detailed overview of current developments and future directions for the CODEX-b detector, which aims to detect long-lived particles beyond the Standard Model. We summarize the scientific motivation for this detector, advances in our suite of simulation and detector optimization frameworks, and examine expected challenges, costs, and timelines in realizing the full detector. Additionally, we describe the technical specifications for the smaller-scale demonstrator detector (CODEX- $\beta$ ) we have installed in the LHCb experimental cavern.

## CONTENTS

I. Introduction and objectives	1
II. Scientific context	2
A. Minimal models	2
B. Complete models	3
III. Tools and Methodologies	4
A. Baseline design and principles	4
B. Fast simulation and optimization frameworks	4
C. Informed design principles and drivers	4
D. Backgrounds and simulation	5
IV. Readiness and expected challenges	6
A. Detector location and representative designs	6
B. Detector technologies	6
V. Timeline	7
VI. Construction and operational costs	8
VII. CODEX- $\beta$	8
A. Goals	8
B. Design and status	9
C. Software development and LHCb integration	10
VIII. Conclusions	10
IX. Acknowledgments	11

## I. INTRODUCTION AND OBJECTIVES

The primary LHC experiments (ATLAS, CMS, LHCb, ALICE) are scheduled to collect data until at least 2040. A core component of the (HL-)LHC program is searches for dark or hidden sectors beyond the Standard Model (BSM), which may be probed in many generic BSM scenarios via searches for displaced decays-in-flight of exotic long-lived particles (LLPs). In the Standard Model (SM), LLPs such as the  $K_L^0$ ,  $\pi^\pm$ , neutron and muon arise via suppressions from scale hierarchies ( $m_W \gg \Lambda_{\text{QCD}}$ ), loop and phase-space suppressions and/or the smallness of one or more CKM matrix elements. LLPs can arise similarly and ubiquitously in BSM scenarios featuring *e.g.*, Dark Matter, Baryogenesis, Supersymmetry, or Neutral Naturalness.

ATLAS, CMS, and LHCb have vibrant LLP search programs that draw on the expertise of analysts, detector specialists, and theorists [1]. Typically, both ATLAS and CMS have non-systematics-limited sensitivities for LLPs that are relatively heavy ( $m \gtrsim 10$  GeV), while backgrounds and trigger challenges strongly limit the reach for light LLPs due to the complicated environment inherent to a high-energy, high-intensity hadron collider; there are, however, some exceptions, *e.g.*, refs. [2, 3]. In the case of LHCb, these difficulties are somewhat offset by its high-precision Vertex Locator (VELO), but LLP sensitivity is nonetheless restricted to relatively short lifetimes and production at low center-of-mass energies; sensitivity to LLPs produced in, *e.g.*, exotic Higgs or  $B$  decays can be similarly limited, especially for  $c\tau \gtrsim 1$  m. Similar considerations apply to FASER, which leverages a very large amount of passive shielding in the very forward regime. Thus, to achieve comprehensive coverage of the full LLP parametric landscape, one or more high volume, *transverse* LLP detectors are needed. The complementarity of these transverse detectors is shown in fig. 1.

**CODEX-b (“Compact Detector for EXotics at LHCb”)** is a special-purpose detector proposed to be installed near and transverse to the LHCb interaction point (IP8) in order to search for displaced decays-in-flight of exotic LLPs [4–6]. The core advantages of CODEX-b are

- competitive sensitivity to a broad array of BSM LLP scenarios, exceeding or complementing the sensitivity of existing or proposed detectors;
- a zero background environment in an accessible experimental location with many of the necessary services already in place;
- the possibility to tag events of interest within the LHCb detector (independent of the LHCb physics program); and
- its compact size and use of existing technology and infrastructure, leading to a modest cost.

Extensive studies of CODEX-b over a large range of different LLP production and decay mechanisms can be found in the Expression of Interest [5] and are briefly summarized below.

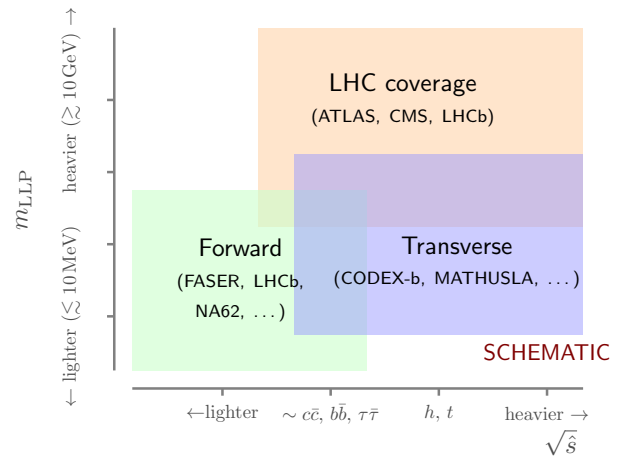


**FIG. 1:** Complementarity of different experiments searching for LLPs [5].

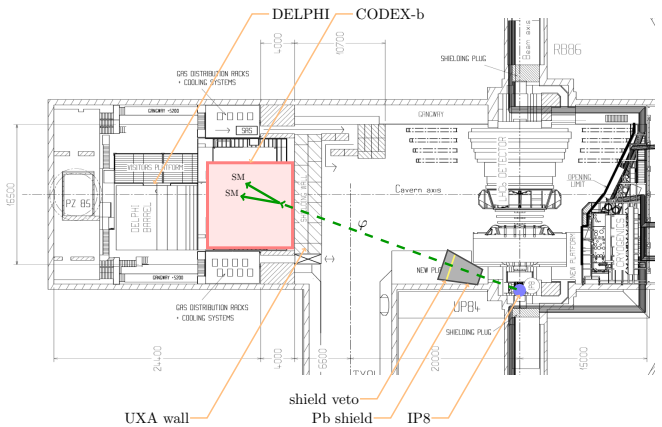


**FIG. 2:** Top view layout of the LHCb experimental cavern UX85 at point 8 of the LHC, overlaid with a schematic of the baseline CODEX-b detector. Adapted from ref. [4].

The proposed CODEX-b detector location is roughly 25 meters from IP8, and the baseline geometry of the detector comprises a fiducial volume of  $10 \times 10 \times 10 \text{ m}^3$ , as shown in fig. 2. Backgrounds are controlled by passive shielding provided by a combination of existing passive shielding (the concrete UXA radiation wall) and an array of active vetoes and passive shielding to be installed adjacent to IP8. A smaller proof-of-concept demonstrator detector, CODEX- $\beta$ , has been installed in the proposed location of CODEX-b, shielded only by the existing wall.

The remainder of this document is structured as follows. We review the scientific context of CODEX-b, including motivation and physics reach in section II. Our methodology towards a successful experiment is described in section III, including simulation and optimization tools and the status of background simulations. Section IV is devoted to the readiness and expected challenges to make CODEX-b a reality, including a discussion of the features and constraints on realistic detector geometries and their performance. Sections V and VI

outline the timeline and costs, respectively. Finally, section VII describes the status of the CODEX- $\beta$  demonstrator detector. We conclude in section VIII.

## II. SCIENTIFIC CONTEXT

Discussed in detail in ref. [5], the physics case for CODEX-b is motivated by the very broad class of models that may be probed through LLP searches: almost any model that features a hierarchy of mass scales, loop suppression, and/or small couplings may have an LLP in its spectrum of states. The broad array of possible LLP signatures, however, raises the problem of how to achieve comprehensive coverage of the theory landscape; this can only be addressed with a set of complementary experiments and searches. The physics case of CODEX-b may be understood via two complementary approaches, studying:

1. *Minimal models*: These are simple SM extensions containing a single new particle that is neutral under all SM gauge interactions. Such simplified models have limited predictive power and physical interpretation, but are good representatives of more complicated ultraviolet completions that address one or more open problems of the SM. This approach motivated the set of benchmark models developed during the Physics Beyond Colliders (PBC) effort [7].
2. *Complete models*: These are more complex realizations that address one or more of the open problems in the SM, including, *e.g.*, the hierarchy problem, baryogenesis, and dark matter.

In the remainder of this section, we briefly summarize the sensitivities under these two approaches for the CODEX-b baseline design presented in section III A; the performance of this design, accounting for tracking and vertex reconstruction efficiencies, is characterized in section IV along with the relative performance of more realistic detector configurations.

### A. Minimal models

The symmetries of the SM restrict the possible couplings through which a new, neutral state may interact with the SM sector. A simple classification is thus possible through the spin of the new state. One typically considers a scalar ( $S$ ), pseudo-scalar ( $a$ ), a fermion ( $N$ ) or a vector ( $A'$ ), where each allows for a handful of dimension-4 and/or 5 operators:

$$\text{Abelian hidden sector: } F_{\mu\nu}F'^{\mu\nu}, \quad hA'_\mu A'^\mu \quad (1a)$$

$$\text{Dark Higgs: } S^2 H^\dagger H, \quad SH^\dagger H \quad (1b)$$

$$\begin{aligned} \text{Axion-like particles: } \quad & \partial^\mu a \bar{\psi} \gamma_\mu \gamma_5 \psi, \quad aW_{\mu\nu} \tilde{W}^{\mu\nu}, \\ & aB_{\mu\nu} \tilde{B}^{\mu\nu}, \quad aG_{\mu\nu} \tilde{G}^{\mu\nu}. \quad (1c) \end{aligned}$$

$$\text{Heavy neutral leptons: } \tilde{H} \bar{L} N \quad (1d)$$

Here  $F'^{\mu\nu}$  represents the field strength operator to the vector field  $A'$ ;  $H$  the SM Higgs doublet;  $h$  the physical, SM Higgs boson;  $L$  the SM lepton doublets;  $\psi$  any SM fermion; and  $B^{\mu\nu}$ ,  $W^{\mu\nu}$  and  $G^{\mu\nu}$  the field strengths of the SM hypercharge,  $SU(2)$  and strong forces, respectively. We also allow for scenarios where a different operator is responsible for the production and decay of the LLP, as summarized below. Finally, we generally use the definitions and conventions specified in ref. [5].

The **Abelian hidden sector** model [8–10] involves just one additional, massive  $U(1)$  gauge boson ( $A'$ ) and its corresponding Higgs boson ( $H'$ ). The  $A'$  and the  $H'$  mix with, respectively, the SM photon and the SM Higgs. If the latter is heavier than the SM Higgs, it decouples from the phenomenology, leaving behind the operators in eq. (1a) in the low-energy effective theory. Production of the  $A'$  occurs through the  $hA'_\mu A'^\mu$  operator, while the  $A'$  decay proceeds via kinetic mixing  $F_{\mu\nu}F'^{\mu\nu}$ . The production and decay rates of the  $A'$  are therefore controlled by independent parameters. The top left plot of fig. 9 shows the reach of CODEX-b for a light  $A'$  mass.

The **dark Higgs** or Higgs portal simplified model involves the maximally minimal addition of a single, real scalar degree of freedom ( $S$ ) that couples to the SM Higgs. The model has three free parameters: the mass ( $m_S$ ), the sine of the mixing angle with the Higgs ( $\sin \theta$ ), and the mixed quartic coupling with the Higgs ( $\lambda_D$ ). The mixing angle controls the lifetime of  $S$  as well as the production rate, which is dominated by exotic  $b$ -hadron decays. When non-zero,  $\lambda_D$  enables pair production of  $S$  both in exotic Higgs and  $b$ -hadron decays. LHCb already has sensitivity to this model [11, 12], but CODEX-b would greatly extend the reach into the small-coupling/long lifetime regime, see the bottom row of fig. 9.

**Axion-like particles** (ALPs) couple to SM fields through dimension-5 operators (1c), which can be generated in a broad range of BSM scenarios. ALPs tend to be light when generated via the breaking of approximate Peccei-Quinn-like symmetries, and their suppressed couplings make them natural LLP candidates. Long-lived ALPs may be abundantly produced at the LHC via their couplings to quarks and/or gluons, through several mechanisms, including: production during hadronization; production from hadron decays via neutral pseudoscalar meson mixing; and production from flavor-changing neutral-current decays of strange or  $b$ -hadrons. In addition, for transverse LLP experiments such as CODEX-b, of particular importance for gluon-coupled ALPs is production by emission in the parton shower. This can lead to substantial enhancements in sensitivity. The projected ALP sensitivity of CODEX-b for gluon-coupled ALPs is shown in the top-right plot of fig. 9 and for fermion-coupled ALPs can be found in ref. [5].

**Heavy neutral leptons** (HNLs) couple to the SM via the marginal lepton Yukawa operators in eq. (1d), or

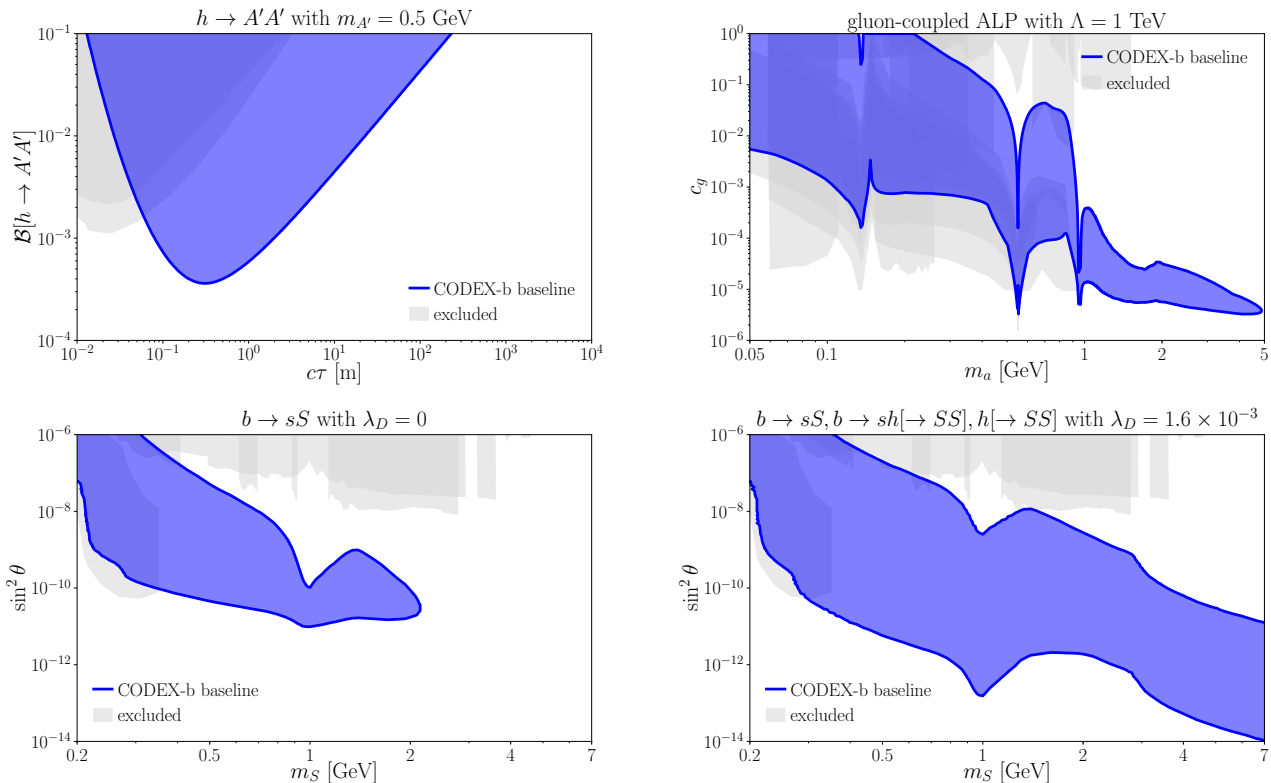


**FIG. 3: (top right)** Baseline CODEX-b reach for  $h \rightarrow A'A'$ . **(top left)** Gluon-coupled axion-like-particle reach. **(bottom)** Simplified dark Higgs model reach with the mixed quartic coupling  $\lambda_D$  chosen such that (left)  $\mathcal{B}[h \rightarrow SS] = 0$  and (right)  $\mathcal{B}[h \rightarrow SS] = 0.01$ . Plots modified from ref. [5] with updated exclusion limits [2, 13–15].

may arise in many simplified NP models involving higher-dimensional operators. These may include explanations for the neutrino masses or theories of dark matter, among others (see below). UV completions of SM-HNL operators imply an active-sterile mixing  $\nu_\ell = U_{\ell j} \nu_j + U_{\ell N} N$ , where  $N$  is the HNL, and the active-sterile mixing  $U_{\ell N}$  is an extended Pontecorvo–Maki–Nakagawa–Sakata (PMNS) neutrino mixing matrix element. The projected HNL sensitivities of CODEX-b for single-flavor mixing with the  $\mu$  and  $\tau$  neutrinos can also be found in ref. [5].

## B. Complete models

Here we review a few examples of complete models featuring LLPs that aim to explain open problems, such as the hierarchy problem, baryogenesis, or the origin of dark matter, that CODEX-b has the potential to discover. For more details, see ref. [5].

Models of **R-parity violating (RPV) supersymmetry** feature light neutralinos, produced through exotic  $B$ ,  $D$ , or  $Z$  decays, that CODEX-b could discover [16, 17]. The sensitivity is approximately independent of the flavor structure of the RPV coupling(s), so long as the net branching ratio to at least two charged tracks is not suppressed.

In **relaxion models** [18], the light scalar  $S$  in the dark

Higgs model stabilizes the electroweak scale [19, 20].

**Neutral Naturalness** models [21, 22] build on the Twin Higgs paradigm [23, 24] that aims to alleviate the SM hierarchy problem. Several versions of these models [22, 25] produce LLPs in exotic Higgs decays.

In many dark matter (DM) models, additional, unstable particles beyond the (meta)stable DM itself are needed to achieve the observed DM relic density. In many cases, these extra particles may be LLPs, detectable at CODEX-b. For example, CODEX-b would be sensitive to **inelastic DM** models [26, 27] that produce very soft, displaced signatures in collider experiments [28]. DM models with **sterile co-annihilation** [29] exhibit phenomenology comparable to the dark Higgs simplified benchmark. **Asymmetric DM** models [30–32] and **Strongly Interacting Massive Particles (SIMPs)** [33–36] implicate the GeV scale, and can contain additional LLP states in the dark sector that could be discovered at CODEX-b. In **Freeze-in models** [37], the DM is never in equilibrium with the SM, which enforces very feeble couplings. These models similarly generically predict LLPs that could be accessible to CODEX-b.

Certain models of baryogenesis rely on out-of-equilibrium decays in the early universe and predict LLPs: **WIMP baryogenesis** is such an exam-

ple [38, 39]. The baryon asymmetry can also be generated through **indirect CP-violation** from heavy flavor baryons [40, 41]. These models predict exotic  $b$ -hadron decays to LLPs, which may be detectable at CODEX-b.

Finally, **HNLs** may arise in explanations for the neutrino masses [42], the  $\nu$ MSM [43, 44], DM models [45], or models which aim to address lepton flavor universality anomalies [46–48].

### III. TOOLS AND METHODOLOGIES

#### A. Baseline design and principles

The baseline detector configuration considered in refs. [4, 5] comprised sextet resistive plate chamber (RPC) panels on the six outer faces of the  $10 \times 10 \times 10$  m<sup>3</sup> cubic detector volume, along with four uniformly-spaced internal RPC triplet stations along the  $x$  axis (in beam-line coordinates). This cubic volume is located at  $x = [26, 36]$  m (transverse),  $y = [-7, 3]$  m (vertical) and  $z = [5, 15]$  m (forward) with respect to IP8. The proposed tracking technology for CODEX-b follows the ATLAS phase-II RPC design [49], so that tracking stations will be composed of arrays of  $1.03 \times 1.88$  m<sup>2</sup> triplet RPC modules, supported by a structural aluminum frame. The sensitivity curves of fig. 9 apply to the baseline detector configuration, assuming 100% LLP vertex reconstruction efficiency. In practice, realistic configurations can achieve vertex reconstruction efficiencies of 40–90%, which amount to small shifts in the logarithmic parameter spaces shown in fig. 9.

In general, an idealized LLP detector design seeks:

1. **Optimal signal sensitivity:** Ensuring the track acceptance is high and instrumentation is capable of reconstructing LLP decay vertices with high efficiency in any given fiducial volume.
2. **Background suppression:** Requiring passive shielding of primary backgrounds, combined with active vetoes for production of secondary backgrounds in the shielding material (primarily by muons); see section III D.

Based on these drivers, the design principles of the baseline configuration were informed by a very conservative approach, which included: (a) a hermetic design to maximally capture signal tracks, veto incoming muons, and veto potential soft cavern backgrounds and (b) a substantial number of internal tracking stations to ensure hits as close as feasible to the decay vertex and thus high track and vertex resolution.

While the baseline design was shown to permit high vertex reconstruction efficiencies over a broad range of portals [4], it requires a very large amount of instrumented surface: a total of  $800 \times 2$  m<sup>2</sup> RPC triplet panels. The production of the required amount of tracking surface poses a significant challenge, both with respect to the short production timescales and with respect to costs and installation time. Moreover, as dis-

cussed in section IV, engineering and technical coordination constraints in the nominal CODEX-b location preempt the possibility of hermetic RPC coverage (though simpler technologies such as scintillator may be possible for the purpose of vetoes). Thus, relaxing the conservative approach and assumptions for the baseline design is necessary.

#### B. Fast simulation and optimization frameworks

To develop more realistic detector design principles and explore the relaxation of the conservative baseline approach, the CODEX-b collaboration has developed a versatile fast simulation framework [50]. This enables rapid simulation of the response to variations in the detector geometry and layouts, with respect to various benchmark LLP production and decay channels, across a range of LLP masses and lifetimes. The studied benchmark scenarios are selected to address a core challenge in optimizing LLP detector design: the broad range of BSM scenarios that may be probed leads to many well-motivated signal morphologies, with widely differing efficiencies and acceptances. For instance, the LLP boost distribution and decay products vary significantly between the dark-Higgs-portal, and the ALP and Abelian-hidden-sector benchmark models mentioned in section II A.

In addition, CODEX-b has developed a deterministic optimization framework [50] based on a combination of set theoretic and branch-and-bound methods. This framework is capable of optimizing, in linear time, exponentially large sets of detector configurations in the nominal  $10 \times 10 \times 10$  m<sup>3</sup> volume subject to realistic engineering or vertex-reconstruction constraints. Simple hit density estimators are also identified that tend to be excellent estimators for systematically optimized configurations. As an example, in fig. 4 we show the relative vertex reconstruction efficiencies as a function of the number of panels, generated by this estimator, for eleven different benchmarks. The notable negative curvature for most benchmarks indicates that large reductions in the number of RPC panels, and thus the elimination of hermetic coverage, are typically possible while maintaining good LLP vertex reconstruction efficiencies.

#### C. Informed design principles and drivers

The core lesson of these optimization studies is that non-hermetic configurations for CODEX-b exist that can attain good sensitivity over the space of LLP scenarios while reducing the required amount of tracking layers by an  $\mathcal{O}(1)$  factor. This, in turn, permits a significant reduction of the forecasted costs, construction, and installation times for the experiment.

Core drivers for CODEX-b design principles under this informed approach comprise:

1. **Geometric acceptance:** sextet RPC tracking

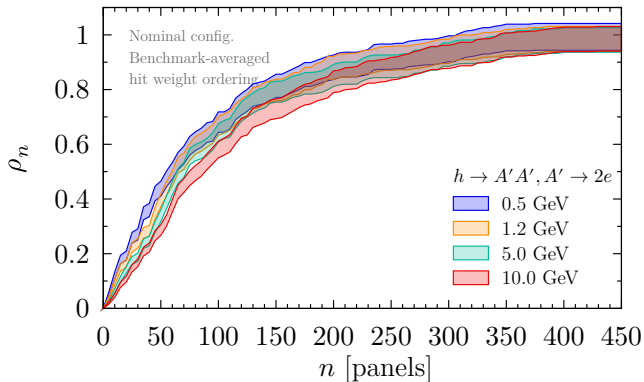


**FIG. 4:** Example relative vertex reconstruction efficiencies ( $1\sigma$  CL bands) versus number of panels [50]. All uncertainties are from the finite statistics of the simulated samples.

layers are required on the entire  $x = 36$  m back face, but far fewer or no RPCs may be required in practice on the  $z = 5$  m near face, or the  $y = 3$  m top or  $y = -7$  m bottom faces.

2. **Vertex resolution:** Good reconstruction resolution of an LLP decay vertex requires at least six hits per track. For areas where only external triplet rather than sextet layers are possible, adjacent triplet internal layers may be required to ensure acceptable track resolution. Internal layers and external sextets are otherwise minimized.
3. **Backgrounds:** Production of secondary particles in the shielding material (primarily) by muons motivates active veto layers on the front  $x = 26$  m face of the detector. Vetoing soft cavern backgrounds may still require hermetic coverage of the detector volume. However, because vetoing backgrounds requires good efficiency rather than hit resolution, this may be achieved with cheaper and simpler scintillator technologies, rather than RPCs.

In all simulations of the vertex reconstruction efficiencies for designs informed by these principles, we also require (a) a minimum track threshold of 600 MeV because of expected multiple rescattering of softer tracks; (b) tracking hits must be separated by at least 2 cm on any given layer, corresponding to the finite RPC hit resolution; (c) an LLP decay vertex resolution of 10 cm, *i.e.*, at least two reconstructed tracks must pass within 10 cm of each other.

#### D. Backgrounds and simulation

Collisions at IP8 produce a large flux of background primary hadrons and leptons. Of these, primary neutral LLPs, *e.g.*, (anti)neutrons and  $K_L^0$ 's, can enter the detector and decay or scatter into tracks resembling a signal decay. Suppression of these primary-hadron fluxes can be achieved with passive shielding material: for a shield of thickness  $L$ , the background flux suppression

$\sim e^{-L/\lambda}$  where  $\lambda$  is the material nuclear interaction length. Background flux rate studies have been performed with GEANT4 [51] and considering various interaction lengths, reaching an optimal zero-background baseline CODEX-b design [5] with 3 m of concrete in the UXA radiation wall, corresponding to  $7\lambda$  of shielding and supplemented with 4.5 m ( $25\lambda$ ) of Pb shielding.

The large amount of shielding material may act in turn as a source of neutral LLP secondaries, produced mainly by scattering of muons or neutrinos. The most concerning neutral secondaries are produced  $< 1$  m from the far side of the shield by muons that slow down and stop before reaching the detector itself. Such muons are invisible to the detector, while their neutral secondaries, such as  $K_L^0$ 's, may reach the detector volume.

Refs. [4, 5] have shown that this problem may be solved with an active veto layer in the shield itself, located to sufficiently veto most muons that produce secondaries, but not so close to the IP that all events are vetoed. Detailed simulations of the setup involve careful treatment of the primary background fluxes at the interaction point, folded into a special GEANT4 simulation of shielding sub elements — usually  $\sim 1$  m thick slices of shielding material — that encode the propagation and secondary production of dozens of different background particles species, over a large range of energies.

As for the baseline design, the simulation makes a series of conservative assumptions:

- Angular distribution of particle scattering is not exploited; all particles scattered within  $23^\circ$  of the forward direction, corresponding to the approximate angular acceptance of the detector, are retained.
- Detector response to neutral secondary particles decaying to charged particles is assumed to be 100%.
- Longer path lengths from non-zero angles of incidence on the shield wall are not included.
- The active veto is implemented in a single layer and does not use tracking information.

Relaxing these simulation assumptions would allow for the study of segmented veto layers that are able to exploit directionality to more efficiently veto background fluxes. Further, simulation of the detector response to background fluxes can improve understanding of likely background-rejection efficiencies. Both aspects may be studied with the tools already being developed for the optimization studies in section III B, to reduce, possibly substantially, the required amount of lead shielding.

As mentioned earlier, a salient feature of the CODEX-b proposal is to trigger on events with an “interesting” pattern of hits in both CODEX-b and the main LHCb detector. Details of the cavern infrastructure geometry and the LHCb magnetic field must be included in the simulation. Backgrounds due to processes other than proton-proton collisions at the LHCb interaction point, known as the LHC machine-induced background (MIB), also occur. To accommodate these, a full simulation including

LHCb, CODEX-b/CODEX- $\beta$ , cavern infrastructure, and MIB, is being developed. Details on the full simulation for CODEX- $\beta$  are presented in section VII C and a preliminary setup for Run 1/2 was described in ref. [6]. This is now being extended to Run 3 data-taking conditions and the CODEX- $\beta$  installation.

The CERN radiation group has placed a battery-operated radiation monitor in the UX85A-D barrack region for Run 3 data taking. This monitor complements the charged background flux measurements of ref. [6], and those that will be measured by CODEX- $\beta$ , since the monitor is sensitive to thermal neutrons that are difficult to simulate.

#### IV. READINESS AND EXPECTED CHALLENGES

##### A. Detector location and representative designs

The proposed detector geometry and location will be primarily informed by the CODEX- $\beta$  demonstrator but is also constrained by engineering and logistical considerations, which are the subject of ongoing deliberations between the LHCb and CODEX-b collaborations. The simulation and optimization framework described in section III B may be used in the development of a realistic design for the full CODEX-b detector, once the engineering constraints in the cavern are fully defined. The main engineering challenges typically involve the integration of existing architecture in the UXA cavern with the services and mechanical supports required by the detector. The difficulty of overcoming these challenges will influence the ultimate selection of location and detector geometry.

To characterize the range of possibilities that may be considered, we show in fig. 5 three CODEX-b scenarios motivated by the discussion of section III C. These scenarios are still under development and serve only to highlight possibilities that might be available as deliberations continue. Scenario 1 is a minor variation of the baseline design to remove all sextets in favor of RPC triplet modules. Scenario 2 further removes all internal tracking stations except one. Finally, we consider scenario 3 that uses an optimized geometry per sections III B and III C to minimize RPC modules while retaining high sensitivity and vertex resolution. It represents a more opportunistic scenario, in which the location of the RPCs has been adapted to putative constraints from existing infrastructure in the UXA cavern, thus reducing the need to reconfigure the space significantly. The baseline design requires 800 RPC triplet modules, scenario 1 requires 500, and scenario 2 and scenario 3 require 350.

For scenario 3, the sextets could be replaced with triplets and augmented with scintillator panels for similar performance, requiring a total of 250 RPC triplet modules. The CODEX- $\beta$  RPC triplet frame, CX1, could easily be adapted for such a scenario, where the frame is loaded with scintillator and steel, and SiPMs are mounted on the edges through the card slots.

**TABLE I:** Relative  $c\tau$ -averaged vertex reconstruction efficiencies compared to the baseline design, for the three representative CODEX-b scenarios and two benchmark models with representative kinematics (see ref. [50], the signal kinematics, and thus expected efficiencies, for ALP LLPs interpolate between those for the Abelian dark sector “ $h \rightarrow A'A'$ ” and the dark Higgs “ $b \rightarrow sS'$ ” benchmarks.). Uncertainties are from the finite statistics of the simulated samples.

$m_{\text{LLP}}$ [GeV]	scenario		
	1	2	3
<b><math>h \rightarrow A'A', A' \rightarrow 2e</math></b>			
0.5	0.81(3)	0.56(2)	0.80(3)
1.2	0.81(3)	0.55(2)	0.72(3)
5.0	0.86(4)	0.58(3)	0.71(3)
10.0	0.88(4)	0.55(3)	0.75(4)
<b><math>b \rightarrow sS', S' \rightarrow 2e</math></b>			
0.5	0.94(11)	0.61(8)	0.77(9)
1.0	0.94(11)	0.55(7)	0.74(9)
2.5	0.85(10)	0.33(5)	0.53(7)
4.0	0.81(11)	0.22(4)	0.42(6)

In table I, we show the  $c\tau$ -averaged vertex reconstruction efficiencies of each of these variations *relative* to the baseline design performance for two representative kinematic scenarios covering the models of fig. 9; the kinematics of the ALP portal are roughly an interpolation between the kinematics of the dark photon and dark Higgs sectors. The vertex reconstruction efficiencies are determined according to the simulation requirements in section III C. The studied configurations can achieve 50–90% relative vertex reconstruction efficiency with respect to the baseline, even with half the instrumentation. Consequently, a full detector may be realized in the nominal detector location, subject to realistic engineering, cost, time, and other technical constraints, but with performance comparable to the original baseline proposal. Correspondingly, the baseline sensitivity curves shown in this document (and in refs. [4, 5]) serve as plausible approximate upper limits on the sensitivity of the full detector and are not expected to shift significantly.

##### B. Detector technologies

While the RPC design itself is well-established, it is necessary to develop firmware and software to communicate seamlessly between the CODEX-b RPCs, which follow the ATLAS phase-II design, and the LHCb software-only trigger. This is also necessary for the successful deployment of the CODEX- $\beta$  demonstrator and is already underway with an expected completion before the end of 2025; see section VII.

The default gas mixture for the CODEX-b RPCs includes R-134a and SF6 [52], both of which have high Global Warming Potential (GWP). However, ECO65 gas provides a performant alternative [53]. Given the

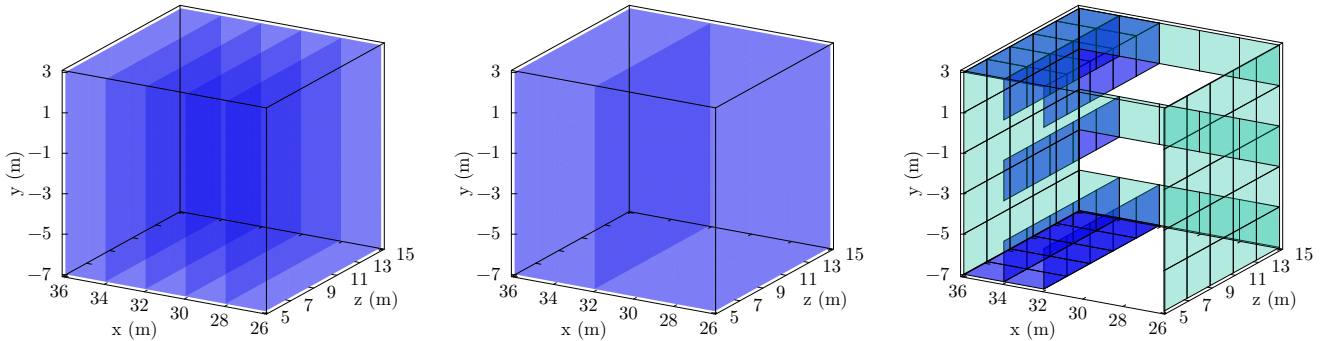


**FIG. 5:** Schematics of CODEX-b design scenarios where triplet (sextet) RPC panels are shown in blue (green): **(left - scenario 1)** baseline configuration with only triplets, **(middle - scenario 2)** baseline configuration with only triplets and a single internal plane, **(right - scenario 3)** an optimized, non-RPC-hermetic configuration subject to cavern constraints.

smaller size of CODEX- $\beta$  [52] and its gas recirculation system, both the default mixture and ECO65 can be tested with minimal environmental impact. Using these tests to establish the RPC performance, it is expected that CODEX-b will also utilize a full recirculation system and an eco-gas mixture.

## V. TIMELINE

The absolute timeline for CODEX-b depends upon CERN approval and the securing of funding. Consequently, a relative timeline is given here based on our experience building CODEX- $\beta$ . The CODEX-b proposal does not require any research and development beyond that for CODEX- $\beta$ , except the near-detector shield and an informed design of the support structure. This shield will consist of lead, with an active scintillator veto, within a movable mechanical support. Members of the CODEX-b collaboration have expertise in scintillator vetoes through the HeRSChE detector for LHCb [54]. The collaboration has also demonstrated mechanical expertise from CODEX- $\beta$  with the development of the CODEX-b module frames, transport carts, and support structure. These mechanics required tolerances within millimeters and were developed in collaboration with civil engineers.

The two primary time-limiting factors are the production of the RPC modules and the installation of the modules in the physical space. With a team of 3 trained personnel, building a single module of 3 RPCs takes approximately 1 week. For CODEX- $\beta$ , our personnel teams consisted of undergraduate students (engineers and physicists), early PhD students (physicists), and post-doctoral researchers (physicists). For CODEX-b, we will recruit effort from a similarly diverse group of personnel. The installation was performed with approximately 5 full-time-equivalent (FTE) for 2 months.

In table II, an estimate is given for the necessary

**TABLE II:** Personnel time estimate for the CODEX-b design scenarios, separated into module building, installation, shield construction, integration with LHCb, and software development. A 20% contingency is included.

task	time [FTE years]		
	baseline	scenario 1	scenario 2/3
RPC modules	55	34	24
detector install	52	32	23
shield	4	4	4
software	12	12	12
LHCb integration	11	11	11
total	134	93	74

FTE years (260 days) to construct and install CODEX-b for the three different scenarios of fig. 5, separated into three large-scale tasks: module building, installation, and shielding. The module building and installation estimates are linearly scaled from CODEX- $\beta$ , and a 20% contingency is included for all estimates. Most of this FTE, roughly 90%, can be provided by student effort as demonstrated with CODEX- $\beta$ . Frame machining is not included in this estimate, but given its straightforward design, frame production would be best achieved via an external vendor. We also expect the RPC module building is an overestimate. Already, the CODEX- $\beta$  team has taken steps towards scaling RPC production.

All three tasks can be performed in parallel. Currently, the CODEX-b collaboration is 22 participating institutes and growing. If each institute provides 3 FTE years over 2 years, then all three scenarios except the baseline can be achieved within this period. If we target the start of 2030 for a full install, then personnel training and material requisitioning need to begin mid-2027. A staged installation could also be performed, as the installation, given appropriate safety measures, could continue during

**TABLE III:** Construction and operational cost estimate for the CODEX-b design scenarios, including a 20% contingency. Numbers in brackets are the standard gas mixture costs (not ECO65).

component	cost [EUR $\times 10^6$ ]		
	baseline	scenario 1	scenario 2/3
RPC modules	14.4	9.0	6.3
power system	3.4	2.1	1.5
gas system	2.7	1.7	1.2
support structure	1.4	0.9	0.6
DAQ	0.7	0.4	0.3
shielding	1.2	1.2	1.2
tooling	1.0	1.0	1.0
gas	26.4	16.5	11.6
(non-eco gas)	3.8	2.4	1.6
total	51.2	32.8	23.6
(non-eco gas)	28.6	18.7	13.8

**TABLE IV:** Cost of a BIS7-S module.

item	units	unit cost	total cost [EUR]
$\eta$ -panel	3	500	1500
$\phi$ -panel	3	500	1500
FE board	36	83	3000
gas gaps	3	1000	3000
frame	1	600	600
cabling	-	-	400
DCT	1	4000	4000
total			15000

LHC operation.

## VI. CONSTRUCTION AND OPERATIONAL COSTS

In table III, we summarize the construction and operational costs for CODEX-b, including a 20% contingency. The estimated personnel requirements are described in section V.

Given our experience developed in building CODEX- $\beta$ , we have a well-defined cost per RPC module of  $1.5 \times 10^4$  EUR based on material purchases. This is the full cost of the module with the component costs detailed in table IV. The cost of the power system, high and low voltage, is also similarly well defined from CODEX- $\beta$ .

For both the gas system and support structure, we have assumed that the cost will scale linearly with the number of RPC modules from the CODEX- $\beta$  cost; this should be an overestimate. The numbers here assume an aluminum support structure, but steel will need to be used in places; this will reduce the cost of the support structure. The DAQ cost is less well defined, given

**TABLE V:** Total neutral and  $K_S^0$  multitrack production during Run 3 in the CODEX- $\beta$  volume for  $\mathcal{L} = 15 \text{ fb}^{-1}$ , requiring  $E_{\text{kin}} > 0.4 \text{ GeV}$  per track [5].

tracks	total	$K_L^0$ contribution
1	$(3.87 \pm 0.11) \times 10^8$	$(2.94 \pm 0.07) \times 10^8$
2	$(4.09 \pm 0.13) \times 10^7$	$(3.74 \pm 0.13) \times 10^7$
3	$(5.96 \pm 1.01) \times 10^5$	$(2.92 \pm 0.45) \times 10^5$
4+	$(9.34 \pm 2.10) \times 10^4$	$(7.03 \pm 1.91) \times 10^4$

that the future cost of the PCIe40 card (see ref. [52]) is unknown. However, we assume the cost of each event-builder server is roughly  $5 \times 10^3$  EUR and each PCIe40 is also  $5 \times 10^3$  EUR, although the latter is almost certainly an overestimate. The cost of the shield is conservatively estimated from the expected cost of the required mechanical structure, lead, and scintillating detector.

The final cost is for the necessary gas over the full lifetime of the detector, assuming a recirculating gas system. This is the primary operating cost, and is also the largest cost of the experiment other than the RPC modules. The gas cost estimate here is scaled from CODEX- $\beta$  usage and assumes the ECO65 gas mixture. If running with the 30% CO2 RPC gas mixture, the gas operational cost is expected to decrease by a factor of roughly 7. Given the importance of the eco-gas mixtures for ATLAS operation, it is expected that the final eco-gas mixture will have a cost significant reduction compared to the current ECO65 mixture.

## VII. CODEX- $\beta$

### A. Goals

The CODEX- $\beta$  detector, described in ref. [52], is a small-scale demonstrator for the full-scale CODEX-b detector. The primary design goal of CODEX- $\beta$  is to validate the key concepts that justify the building and operation of CODEX-b. Specifically:

1. Demonstrate the suitability of the mechanical support required for the RPCs and its scalability to the full CODEX-b detector.
2. Validate the preliminary background estimates from the CODEX-b proposal and the 2018 background measurement campaign [6], including measurement of soft cavern backgrounds, demonstrating that CODEX-b can be operated as a zero-background experiment (see section III D).
3. Demonstrate the seamless integration of the detector with the LHCb readout, so that candidate LLP events in CODEX-b can be tagged with the corresponding LHCb detector information to aid in their interpretation.
4. Demonstrate the suitability of RPCs as a baseline tracking technology for CODEX-b in terms of spatial granularity, hermeticity, and timing resolution.

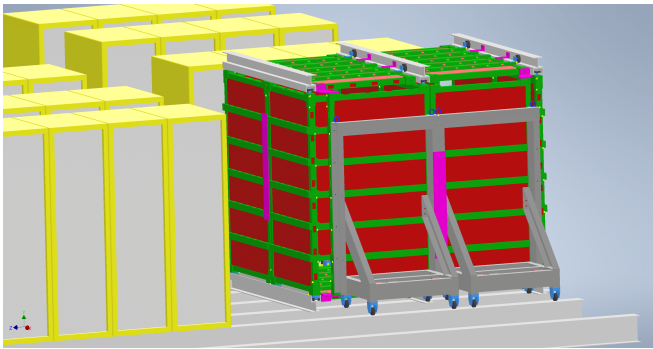


**FIG. 6:** Schematic of CODEX- $\beta$  (green, red, gray) located between the server racks (yellow, gray).

5. Demonstrate an ability to reconstruct known SM backgrounds expected to decay inside UX-85A (the proposed location for CODEX-b and CODEX- $\beta$ ) and validate a full simulation of the LHCb detector and cavern environment with these measured backgrounds.

The demonstrator built our expertise in building and operating RPCs and the development of the data acquisition, simulation, and software needed to operate CODEX- $\beta$  will significantly simplify similar activities needed for CODEX-b.

A powerful tool to calibrate the detector reconstruction and the RPC timing resolution is the measurement of long-lived SM particles decaying inside the detector acceptance. The most natural candidates are  $K_S^0$  mesons. Table V summarizes the expected multitrack production from decay or scattering on air-by-neutral fluxes entering CODEX- $\beta$ , as well as the contribution from just  $K_S^0$  mesons entering the detector. Approximately a few  $\times 10^7$   $K_S^0$  decays to two or more tracks are expected in the CODEX- $\beta$  volume per nominal year of data taking in Run 3, so that CODEX- $\beta$  will have the opportunity to reconstruct a variety of  $K_S^0$  decays. The measurement of the decay vertex and decay product trajectories will allow the boost of the LLP to be reconstructed independently from the time-of-flight information. Moreover, measurements of the distribution of  $K_S^0$  decay vertices can be compared to expectations from the background simulation of the expected  $K_S^0$  boost distribution folded against the  $K_S^0$  lifetime, allowing calibration and validation of our detector simulation and reconstruction. Conversely, one may combine the predicted boost distribution and measured vertex distribution to extract the  $K_S^0$  lifetime itself.

### B. Design and status

As shown in the schematic of fig. 6, CODEX- $\beta$  comprises a  $2 \times 2 \times 2$  m<sup>3</sup> cube with an additional interior face. Each face contains two modules, each housing a stacked triplet of  $2 \times 1$  m<sup>2</sup> RPCs integrated into a self-contained mechanical frame. A total of  $(6+1) \times 2 \times 3 = 42$

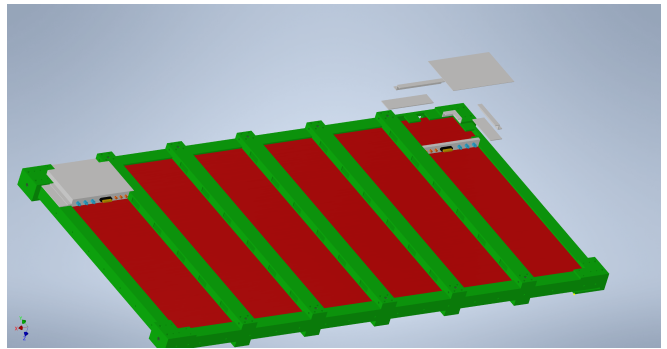


**FIG. 7:** Schematic of a CODEX- $\beta$  module, including the RPC triplet (red), support frame (green), and service boxes (gray).

RPC singlets are integrated into a total of 14 modules. A schematic of the mechanical frame, specifically designed to withstand the stresses of handling and mounting, is shown in the top diagram of fig. 7.

The location for CODEX- $\beta$ , as well as planned CODEX-b locations, is challenging to access. Therefore, the frame has been designed to be highly modular and can be assembled with just fastening hardware and no welding. One of the key installation features is rolling support carts, which can be used to move the modules to the frame. The final four modules remain in carts, allowing access to the interior of the detector.

The base element of a module is the singlet RPC, identical to the BIS7 RPCs used in the ATLAS Upgrade experiment [55]. Each module contains three independent singlets, a triplet, which provide a three-point track and operate in a self-trigger mode, obviating the need for any external reference system for cosmic muon detection.

To form a full  $2 \times 2$  m<sup>2</sup> face of the CODEX- $\beta$  cube, two modules are placed side-by-side along their  $\phi$  sides such that the readouts are on the opposite outer edges of the module. This maintains the hermeticity of the detector. For the full CODEX-b design, internal routing of the readout cables may be modified for the sequential positioning of more than two modules.

At the time of submission for this document, the CODEX- $\beta$  detector is installed in its location, see fig. 8. The power and gas services are prepared, and a test data acquisition system is installed to verify the efficiencies and the noise level of each RPC *in situ*. All components for the final data acquisition have been designed and are in the process of being procured. The realization of the full reconstruction and the integration into the LHCb readout require dedicated firmware modifications to the front-end and the LHCb data acquisition. These developments, together with the necessary software amendments in the LHCb framework to allow simultaneous readout, are in progress.

With the beginning of the data taking in 2025, we will first commission the hardware with a test data acquisition, validating the performance of the RPCs and mea-



FIG. 8: Physical installation of CODEX- $\beta$  at IP8.

sure background rates with the chambers *in situ*. Once the final data acquisition system is ready, reconstruction and integration milestones can be verified.

### C. Software development and LHCb integration

A dedicated full software framework for CODEX- $\beta$  is now under preparation. This framework covers the following:

1. **CODEX- $\beta$  event definition:** New data banks and encoders to accommodate the response from the RPC readout into the LHCb DAQ will be developed.
2. **Simulation:** New Pythia settings, as well as both the CODEX- $\beta$  geometry and a parameterization of the existing concrete wall, will be implemented to simulate any material interaction.
3. **Digitization:** All tracks from simulation should be digitized to emulate the RPC readout, matching the response format from real data acquisition.
4. **Reconstruction:** A decoder and algorithms for track reconstruction will be developed, storing data into a suitable format for data analysis.
5. **Data analysis:** Dedicated analysis tools will be developed for offline data analysis and online data quality assessment during data-taking, in an automated way.

Items 1 to 3 will be implemented into the LHCb software stack, while 4 and 5 use the output from the previous steps in a standalone manner, decoupled from LHCb software. The complete software framework will be tested and validated before integration into the LHCb software stack.

Before the steps above, the CODEX- $\beta$  readout will be integrated into the LHCb data stream, and we will val-

idate the data acquisition model and its scalability to the full detector. Currently, the CODEX- $\beta$  event definition and digitization are being developed, and should be completed by the end of summer. The integration of CODEX- $\beta$  within the LHCb simulation framework is nearing completion, while the event reconstruction will be performed in parallel with other tasks this summer. Finally, data analysis will be performed during data taking.

## VIII. CONCLUSIONS

Currently, numerous experimental collaborations are working to develop dedicated facilities for studying LLPs, capitalizing on the LHC's production capabilities and luminosity projected for the next twenty years. Within this research landscape, the CODEX-b experiment occupies a distinctive position: it offers a relatively modest-sized, cost-effective solution using established technologies. Its strategic location minimizes staffing requirements while enabling integration with LHCb's existing data acquisition systems. The detector provides competitive or complementary sensitivity for detecting LLPs produced in both transverse and longitudinal directions. Having confirmed most of the fundamental assertions from its 2017 proposal [4], the CODEX-b collaboration is nearly ready to start taking data with the CODEX- $\beta$  demonstrator — laying groundwork for the complete CODEX-b detector's construction and implementation in the late 2020s.

Our current focus centers on commissioning the CODEX- $\beta$  demonstrator to capture a significant portion of Run 3 luminosity at IP8. This collected data will enable precise measurements of both overall background levels in UX-85A and their spatial distribution, informing the optimization of size and configuration for CODEX-b's required active veto shield. Reconstructing SM backgrounds will provide crucial validation for CODEX-b simulations, allowing confident optimization of the spatial and temporal resolution requirements for CODEX-b RPCs, as well as their physical arrangement.

Following completion of CODEX- $\beta$  activities, we will finalize a fully optimized configuration for both CODEX-b and its active shield veto, comprehensive performance specifications for the CODEX-b RPCs, and a detailed mechanical design for the final experiment. Based on these developments, we will create a Technical Design Report and pursue a phased construction and installation approach, leveraging UX-85A's shielded environment that permits work during both operational periods and scheduled LHC maintenance shutdowns.

The HL-LHC holds great potential for the exploration of BSM scenarios involving LLPs. The CODEX-b detector is well-positioned to realize this potential.

## IX. ACKNOWLEDGMENTS

We are grateful for the support we have received from the LHCb collaboration. We thank the technical and administrative staffs at CERN and at other CODEX-b institutes for their contributions to the success of the CODEX-b and CODEX- $\beta$  effort. In addition, we gratefully acknowledge the computing centers and personnel of the Worldwide LHC Computing Grid and other centres for delivering so effectively the computing infrastructure essential to our analyses.

Individuals have received support from the Science and Technology Facilities Council (UK) [grant reference ST/W004305/1] and National Research, Development and Innovation Office (NKFIH) research grant (Hungary) [contract number TKP2021-NKTA-64]. The work of IGFAE members and of CVS is supported by the Spanish Research State Agency under projects PID2022-139514NA-C33 and PCI2023-145984-2. The work of IGFAE members is supported by Xunta de Galicia (Centro singular de investigación de Galicia accreditation 2019-2022), by European Union ERDF; and by the Spanish Ministry of Universities under the NextGenerationEU program. The work of LBNL staff/researchers is supported by the Office of High Energy Physics of the U.S. Department of Energy under contract DE-AC02-05CH11231. The work of the University of Cincinnati personnel is in part supported by the United States National Science Foundation under grant NSF-PHY-220976. The work of the DESY personnel is supported by DESY (Hamburg, Germany), a member of the Helmholtz Association HGF, and by the Deutsche Forschungsgemeinschaft (DFG, German Research Foundation) under Germany's Excellence Strategy – EXC 2121 “Quantum Universe” – 390833306. The work of CVS is supported by Agencia Estatal de Investigación (Spain) through the Ramón y Cajal program RYC2023-043804-I and the Universidade da Coruña-InTalent program.

## REFERENCES

- 
- [1] J. Alimena et al., *Searching for long-lived particles beyond the Standard Model at the Large Hadron Collider*, *J. Phys. G* **47** (2020) 090501, [[1903.04497](#)].
- [2] CMS collaboration, A. Tumasyan et al., *Search for long-lived particles decaying into muon pairs in proton-proton collisions at  $\sqrt{s} = 13$  TeV collected with a dedicated high-rate data stream*, *JHEP* **04** (2022) 062, [[2112.13769](#)].
- [3] CMS collaboration, A. Tumasyan et al., *Search for Long-Lived Particles Decaying in the CMS End Cap Muon Detectors in Proton-Proton Collisions at  $\sqrt{s} = 13$  TeV*, *Phys. Rev. Lett.* **127** (2021) 261804, [[2107.04838](#)].
- [4] V. V. Gligorov, S. Knapen, M. Papucci and D. J. Robinson, *Searching for Long-lived Particles: A Compact Detector for Exotics at LHCb*, *Phys. Rev.* **D97** (2018) 015023, [[1708.09395](#)].
- [5] G. Aielli et al., *Expression of interest for the CODEX-b detector*, *Eur. Phys. J. C* **80** (2020) 1177, [[1911.00481](#)].
- [6] B. Dey, J. Lee, V. Coco and C.-S. Moon, *Background studies for the CODEX-b experiment: measurements and simulation*, [1912.03846](#).
- [7] J. Beacham et al., *Physics Beyond Colliders at CERN: Beyond the Standard Model Working Group Report*, *J. Phys. G* **47** (2020) 010501, [[1901.09966](#)].
- [8] R. M. Schabinger and J. D. Wells, *A Minimal spontaneously broken hidden sector and its impact on Higgs boson physics at the large hadron collider*, *Phys. Rev.* **D72** (2005) 093007, [[hep-ph/0509209](#)].
- [9] S. Gopalakrishna, S. Jung and J. D. Wells, *Higgs boson decays to four fermions through an abelian hidden sector*, *Phys. Rev.* **D78** (2008) 055002, [[0801.3456](#)].
- [10] D. Curtin, R. Essig, S. Gori and J. Shelton, *Illuminating Dark Photons with High-Energy Colliders*, *JHEP* **02** (2015) 157, [[1412.0018](#)].
- [11] LHCb collaboration, R. Aaij et al., *Search for long-lived scalar particles in  $B^+ \rightarrow K^+ \chi(\mu^+ \mu^-)$  decays*, *Phys. Rev.* **D95** (2017) 071101, [[1612.07818](#)].
- [12] LHCb collaboration, R. Aaij et al., *Search for hidden-sector bosons in  $B^0 \rightarrow K^{*0} \mu^+ \mu^-$  decays*, *Phys. Rev. Lett.* **115** (2015) 161802, [[1508.04094](#)].
- [13] CMS collaboration, A. Hayrapetyan et al., *Search for long-lived particles decaying in the CMS muon detectors in proton-proton collisions at  $s=13$  TeV*, *Phys. Rev. D* **110** (2024) 032007, [[2402.01898](#)].
- [14] CMS collaboration, A. Hayrapetyan et al., *Search for long-lived particles decaying to final states with a pair of muons in proton-proton collisions at  $\sqrt{s} = 13.6$  TeV*, *JHEP* **05** (2024) 047, [[2402.14491](#)].
- [15] FASER collaboration, R. Mammen Abraham et al., *Shining light on the dark sector: search for axion-like particles and other new physics in photonic final states with FASER*, *JHEP* **01** (2025) 199, [[2410.10363](#)].
- [16] D. Dercks, J. De Vries, H. K. Dreiner and Z. S. Wang, *R-parity Violation and Light Neutralinos at CODEX-b, FASER, and MATHUSLA*, *Phys. Rev.* **D99** (2019) 055039, [[1810.03617](#)].
- [17] J. C. Helo, M. Hirsch and Z. S. Wang, *Heavy neutral fermions at the high-luminosity LHC*, *JHEP* **07** (2018) 056, [[1803.02212](#)].

- [18] P. W. Graham, D. E. Kaplan and S. Rajendran, *Cosmological Relaxation of the Electroweak Scale*, *Phys. Rev. Lett.* **115** (2015) 221801, [[1504.07551](#)].
- [19] T. Flacke, C. Frugiuele, E. Fuchs, R. S. Gupta and G. Perez, *Phenomenology of relaxion-Higgs mixing*, *JHEP* **06** (2017) 050, [[1610.02025](#)].
- [20] K. Choi and S. H. Im, *Constraints on Relaxion Windows*, *JHEP* **12** (2016) 093, [[1610.00680](#)].
- [21] N. Craig, S. Knapen and P. Longhi, *Neutral Naturalness from Orbifold Higgs Models*, *Phys. Rev. Lett.* **114** (2015) 061803, [[1410.6808](#)].
- [22] N. Craig, A. Katz, M. Strassler and R. Sundrum, *Naturalness in the Dark at the LHC*, *JHEP* **07** (2015) 105, [[1501.05310](#)].
- [23] Z. Chacko, H.-S. Goh and R. Harnik, *The Twin Higgs: Natural electroweak breaking from mirror symmetry*, *Phys. Rev. Lett.* **96** (2006) 231802, [[hep-ph/0506256](#)].
- [24] Z. Chacko, H.-S. Goh and R. Harnik, *A Twin Higgs model from left-right symmetry*, *JHEP* **01** (2006) 108, [[hep-ph/0512088](#)].
- [25] N. Craig, S. Knapen, P. Longhi and M. Strassler, *The Vector-like Twin Higgs*, *JHEP* **07** (2016) 002, [[1601.07181](#)].
- [26] D. Tucker-Smith and N. Weiner, *Inelastic dark matter*, *Phys. Rev. D* **64** (2001) 043502, [[hep-ph/0101138](#)].
- [27] E. Izaguirre, G. Krnjaic and B. Shuve, *Discovering Inelastic Thermal-Relic Dark Matter at Colliders*, *Phys. Rev. D* **93** (2016) 063523, [[1508.03050](#)].
- [28] A. Berlin and F. Kling, *Inelastic Dark Matter at the LHC Lifetime Frontier: ATLAS, CMS, LHCb, CODEX-b, FASER, and MATHUSLA*, *Phys. Rev.* **D99** (2019) 015021, [[1810.01879](#)].
- [29] R. T. D’Agnolo, C. Mondino, J. T. Ruderman and P.-J. Wang, *Exponentially Light Dark Matter from Coannihilation*, *JHEP* **08** (2018) 079, [[1803.02901](#)].
- [30] D. E. Kaplan, M. A. Luty and K. M. Zurek, *Asymmetric Dark Matter*, *Phys. Rev.* **D79** (2009) 115016, [[0901.4117](#)].
- [31] I.-W. Kim and K. M. Zurek, *Flavor and Collider Signatures of Asymmetric Dark Matter*, *Phys. Rev.* **D89** (2014) 035008, [[1310.2617](#)].
- [32] K. M. Zurek, *Asymmetric Dark Matter: Theories, Signatures, and Constraints*, *Phys. Rept.* **537** (2014) 91–121, [[1308.0338](#)].
- [33] Y. Hochberg, E. Kuflik, T. Volansky and J. G. Wacker, *Mechanism for Thermal Relic Dark Matter of Strongly Interacting Massive Particles*, *Phys. Rev. Lett.* **113** (2014) 171301, [[1402.5143](#)].
- [34] Y. Hochberg, E. Kuflik, H. Murayama, T. Volansky and J. G. Wacker, *Model for Thermal Relic Dark Matter of Strongly Interacting Massive Particles*, *Phys. Rev. Lett.* **115** (2015) 021301, [[1411.3727](#)].
- [35] S.-M. Choi, Y. Hochberg, E. Kuflik, H. M. Lee, Y. Mambrini, H. Murayama et al., *Vector SIMP dark matter*, *JHEP* **10** (2017) 162, [[1707.01434](#)].
- [36] S.-M. Choi, H. M. Lee, P. Ko and A. Natale, *Resolving phenomenological problems with strongly-interacting-massive-particle models with dark vector resonances*, *Phys. Rev.* **D98** (2018) 015034, [[1801.07726](#)].
- [37] L. J. Hall, K. Jedamzik, J. March-Russell and S. M. West, *Freeze-In Production of FIMP Dark Matter*, *JHEP* **03** (2010) 080, [[0911.1120](#)].
- [38] Y. Cui and R. Sundrum, *Baryogenesis for weakly interacting massive particles*, *Phys. Rev.* **D87** (2013) 116013, [[1212.2973](#)].
- [39] Y. Cui and B. Shuve, *Probing Baryogenesis with Displaced Vertices at the LHC*, *JHEP* **02** (2015) 049, [[1409.6729](#)].
- [40] D. McKeen and A. E. Nelson, *CP Violating Baryon Oscillations*, *Phys. Rev.* **D94** (2016) 076002, [[1512.05359](#)].
- [41] K. Aitken, D. McKeen, T. Nader and A. E. Nelson, *Baryogenesis from Oscillations of Charmed or Beautiful Baryons*, *Phys. Rev.* **D96** (2017) 075009, [[1708.01259](#)].
- [42] R. N. Mohapatra and J. W. F. Valle, *Neutrino Mass and Baryon Number Nonconservation in Superstring Models*, *Phys. Rev.* **D34** (1986) 1642.
- [43] T. Asaka, S. Blanchet and M. Shaposhnikov, *The  $\nu$ MSM, dark matter and neutrino masses*, *Phys. Lett. B* **631** (2005) 151–156, [[hep-ph/0503065](#)].
- [44] T. Asaka and M. Shaposhnikov, *The  $\nu$ MSM, dark matter and baryon asymmetry of the universe*, *Phys. Lett. B* **620** (2005) 17–26, [[hep-ph/0505013](#)].
- [45] B. Batell, T. Han, D. McKeen and B. Shams Es Haghi, *Thermal Dark Matter Through the Dirac Neutrino Portal*, *Phys. Rev. D* **97** (2018) 075016, [[1709.07001](#)].
- [46] A. Greljo, D. J. Robinson, B. Shakya and J. Zupan,  *$R(D^{(*)})$  from  $W'$  and right-handed neutrinos*, *JHEP* **09** (2018) 169, [[1804.04642](#)].
- [47] P. Asadi, M. R. Buckley and D. Shih, *It’s all right(-handed neutrinos): a new  $W'$  model for the  $R(D^{(*)})$  anomaly*, *JHEP* **09** (2018) 010, [[1804.04135](#)].
- [48] D. J. Robinson, B. Shakya and J. Zupan, *Right-handed neutrinos and  $R(D^{(*)})$* , *JHEP* **02** (2019) 119, [[1807.04753](#)].
- [49] ATLAS collaboration, *Technical Design Report for the Phase-II Upgrade of the ATLAS Muon Spectrometer*, Tech. Rep. CERN-LHCC-2017-017. ATLAS-TDR-026, CERN, Geneva, Sep, 2017.
- [50] T. Gorordo, S. Knapen, B. Nachman, D. J. Robinson and A. Suresh, *Geometry optimization for long-lived particle detectors*, *JINST* **18** (2023) P09012, [[2211.08450](#)].
- [51] GEANT4 collaboration, S. Agostinelli et al., *GEANT4: A Simulation toolkit*, *Nucl. Instrum. Meth.* **A506** (2003) 250–303.
- [52] CODEX-b collaboration, G. Aielli et al., *Technical design report for the CODEX- $\beta$  demonstrator*, [2406.12880](#).
- [53] ATLAS MUON collaboration, G. Proto, *Study of environment friendly gas mixtures for the Resistive Plate Chambers of*

- the ATLAS phase-2 upgrade*, *Nucl. Instrum. Meth. A* **1070** (2025) 170014, [2503.05615].
- [54] K. C. Akiba et al., *The HeRSChE L detector: high-rapidity shower counters for LHCb*, *JINST* **13** (2018) P04017, [1801.04281].
- [55] ATLAS MUON collaboration, L. Massa, *The BIS78 Resistive Plate Chambers upgrade of the ATLAS Muon Spectrometer for the LHC Run-3*, *JINST* **15** (2020) C10026, [2004.12693].
- [56] G. Aielli et al., *The Road Ahead for CODEX-b*, **2203.07316**.

### Appendix A: CODEX-b Main documents

The following are the main documents the CODEX-b collaboration has published.

paper	description
V. V. Gligorov, S. Knapen, M. Papucci and D. J. Robinson, <i>Searching for Long-lived Particles: A Compact Detector for Exotics at LHCb</i> , <i>Phys. Rev. D</i> <b>97</b> (2018) 015023, [ <a href="#">1708.09395</a> ]	Original CODEX-b proposal.
G. Aielli et al., <i>Expression of interest for the CODEX-b detector</i> , <i>Eur. Phys. J. C</i> <b>80</b> (2020) 1177, [ <a href="#">1911.00481</a> ]	Expression of interest.
T. Gorordo, S. Knapen, B. Nachman, D. J. Robinson and A. Suresh, <i>Geometry optimization for long-lived particle detectors</i> , <i>JINST</i> <b>18</b> (2023) P09012, [ <a href="#">2211.08450</a> ]	Geometry optimization paper
G. Aielli et al., <i>The Road Ahead for CODEX-b</i> , <a href="#">2203.07316</a>	CODEX-b snowmass contribution.
CODEX-b collaboration, G. Aielli et al., <i>Technical design report for the CODEX-<math>\beta</math> demonstrator</i> , <a href="#">2406.12880</a>	CODEX- $\beta$ TDR, detailing all details concerning its construction and installation.

### Appendix B: FTE estimation for software and LHCb integration

1. **Integration with LHCb:** since we plan to use the LHCb triggers, we need to integrate CODEX-b with LHCb. Lessons from CODEX- $\beta$  can be recycled, although a team of 2 experts should work 1.5 FTE/y. **This task requires 3 FTE/y.**
2. **CODEX-b ECS and DAQ:** together with the integration in LHCb, we need to develop our data acquisition and experiment control system, to process data from the RPC readout, ensure synchronicity with the LHC and LHCb, and control the experiment. **This task will need a team of 3 experts working 2 FTE/y, for a total of 6 FTE/y.**
3. **Simulation:** A full simulation package should be developed, with PYTHIA/MADGRAPH generators and a complete GEANT4 detector and shielding simulation. This will take a team of 3 people, at least 1 post-doc, working 0.5 years on the generation and 1.5 years on the simulation. Also, the fast simulation should be prepared for general public use, requiring 2 people working 0.5 FTE/y. **This is a total of 7 FTE/y.**
4. **Digitization:** this task should be straightforward and **will require 1 person working 0.5 FTE/y.**
5. **Reconstruction:** this task can be recycled from the work with CODEX- $\beta$ , and **will require 3 people working 0.5 FTE/y, totaling 1.5 FTE/y.**
6. **Data analysis:** dedicated data analysis tools and automated DQM can be recycled from CODEX- $\beta$ , and **will require 2 people working 0.5 FTE/y, totaling 1 FTE/y.**

This leads to the summary of table VI.

**TABLE VI:** Personnel time estimate for CODEX-b software development and integration with LHCb.

task	time [FTE years]		
	baseline	scenario 1	scenario 2
integration with LHCb	3	3	3
CODEX-b ECS and DAQ	6	6	6
DAQ/ECS total	9	9	9
simulation	7	7	7
digitization	0.5	0.5	0.5
reconstruction	1.5	1.5	1.5
data analysis	1	1	1
software total	10	10	10
grand total	19	19	19

## Appendix C: Additional Plots

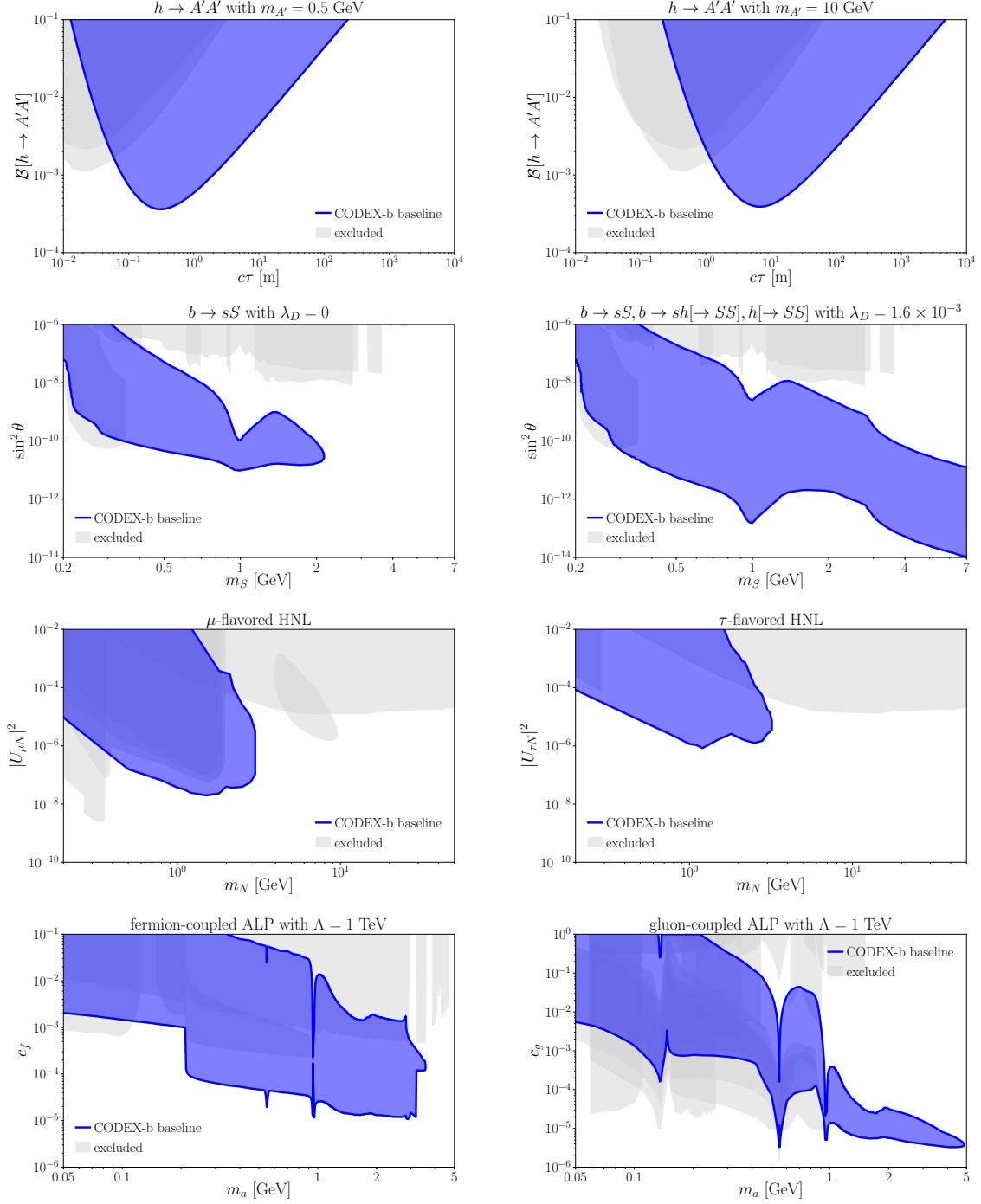


**FIG. 9:** (top) Baseline CODEX-b reach for  $h \rightarrow A'A'$  with two different  $A'$  masses compared to current exclusion limits. (middle upper) Simplified dark Higgs model reach with the mixed quartic coupling  $\lambda_D$  chosen such that (left)  $\mathcal{B}[h \rightarrow SS] = 0$  and (right)  $\mathcal{B}[h \rightarrow SS] = 0.01$ . (middle lower) Reach for (left)  $\mu$ - and (right)  $\tau$ -flavored HNLs. (bottom) Reach for (left) fermion- and (right) gluon-coupled ALPs. Plots modified from ref. [5] with updated exclusion limits [2, 13–15].